Supplements to

"Top-down and bottom-up controls on mountain-hopping erosion: insights from detrital ^{10}Be and river profile analysis in Central Guatemala"

By Gilles Y Brocard, Jane K Willenbring, Tristan Salles, Mickael Cosca, Axel Guttierez, Noé Cacao Chiquín, Sergio Morán-Ical, Christian Teyssier

Content:

Supplement 1. *^{40}Ar/^{39}Ar radiometric dating*

The crushed whole-rock samples were irradiated with standards in 3 separate irradiations at 0.5, 3, and 5 MWh, respectively, in the central thimble position of the USGS TRIGA reactor (Dalrymple et al., 1981), while being rotated at 1 rpm. Following irradiation, the samples and standards were loaded to a stainless steel sample holder with tweezers and then placed into a laser chamber with an externally pumped ZnSe window. The volume of the mostly stainless steel vacuum extraction line, including a cryogenic trap operated at -130°C and two SAES™ GP50 getters (one operated at room temperature, one at 2.2A), is ~450 cm^3. A combination of turbo molecular pumps and ion pumps maintains steady pressures at < 1.33 10^{-7} Pa within the extraction line. Samples were incrementally heated in steps of 90 seconds, by controlled power output of a 50W CO_2 laser equipped with a beam-homogenizing lens, which results in a uniform energy distribution over the entire sample surface. Any sample gas that was released during laser heating was exposed to the cryogenic trap and further purified for an additional 120 seconds by exposure to both the cryogenic trap and the SAES getters. The sample gas was expanded into a Thermo Scientific ARGUS VI™ mass spectrometer where argon isotopes were analyzed simultaneously using four faraday detectors (^{40}Ar, ^{39}Ar, ^{38}Ar, ^{37}Ar) and an ion counter (^{36}Ar). Detector calibration was carried out using a fixed reference voltage on the faraday detectors. The ion counter was calibrated relative to the faraday detectors by regular air pipette measurements, and the detector discrimination was monitored by the ^{40}Ar/^{39}Ar ratios of Fish Canyon sanidine measurements. Following 10 minutes of data acquisition, time zero intercepts were fit to the data (using parabolic and/or linear best fits) and corrected for backgrounds, detector inter-calibrations, and nucleogenic interferences. The computer program Mass Spec (A. Deino, Berkeley Geochronology Center) was used for data acquisition, age calculations, and plotting. The ^{40}Ar/^{39}Ar ages reported in Supplementary Table SI-x are calculated assuming an age of 28.201 ± 0.046 Ma for the Fish Canyon sanidine (Kuiper et al., 2008), using the decay constants of Min et al. (2000), and an atmospheric ^{40}Ar/^{36}Ar of 298.56 ± 0.31 (Lee et al., 2010). Laser fusion of more than ten individual Fish Canyon Tuff sanidine crystals at each closely monitored position within the irradiation package resulted in neutron flux ratios reproducible to ≤ 0.25% (2σ). Isotopic production ratios were determined from irradiated CaF_2 and KCl salts. For this study the following values were measured: (^{36}Ar/^{37}Ar)Ca = (2.4 ± 0.05)10^{-4}; (^{39}Ar/^{37}Ar)Ca = (6.59 ± 0.10)10^{-4}; and (^{38}Ar/^{39}Ar)K = (1.29 ± 0.03)10^{-2}. Cadmium shielding during irradiation prevented any measurable (^{40}Ar/^{39}Ar)K. For the calculation of the plateau ages we required three or more consecutive heating steps that released ≥ 50% of the total ^{39}Ar and also had statistically (2σ) indistinguishable ^{40}Ar/^{39}Ar ages.

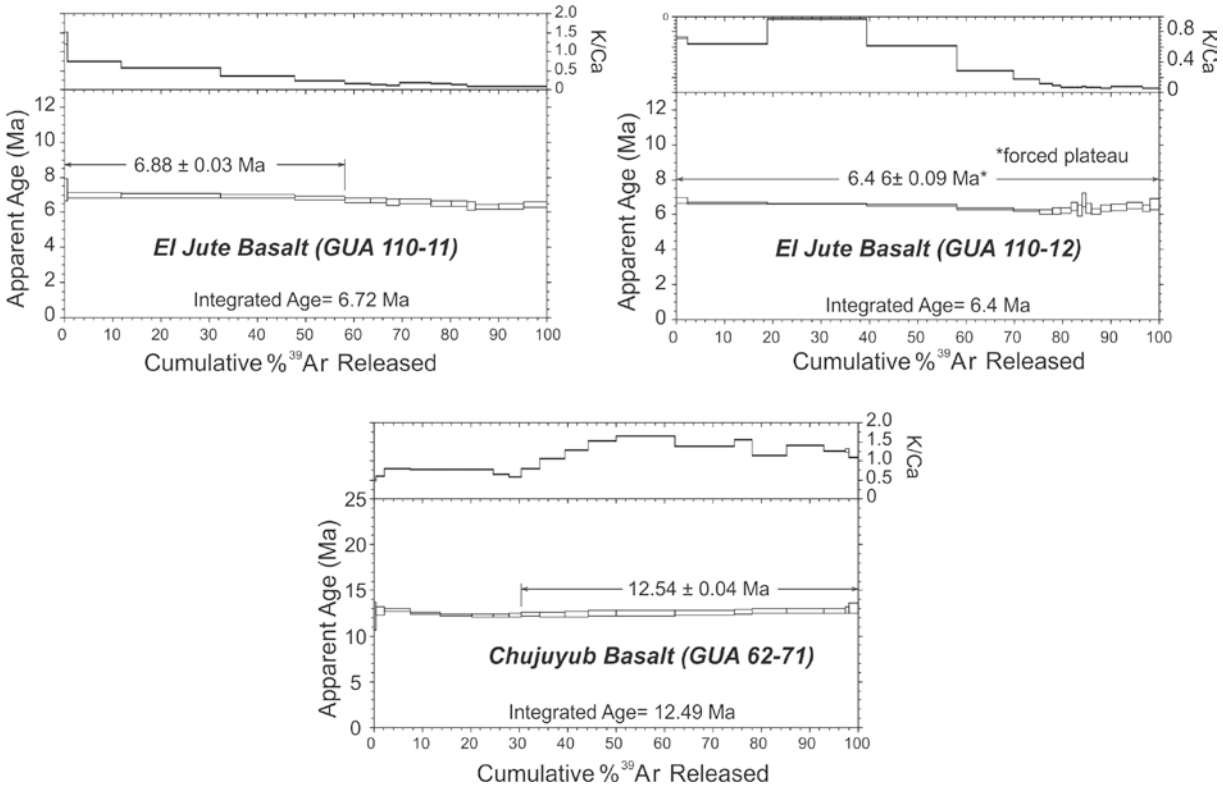

Figure S1-1. Heating step releases and statistics for the calculation of whole rock basalt $^{40}Ar/^{39}Ar$ ages.

Table SI-y. $^{40}Ar/^{39}Ar$ results

CO_2 laser	Relative Isotopic Abundances (x 10^{-13}A)										Derived Results						
Power	^{40}Ar		^{39}Ar		^{38}Ar		^{37}Ar		^{36}Ar		^{39}Ar Mol	^{39}Ar %	Ca/K		$\%^{40}Ar^*$	Age (Ma)	
(Watts)	±1σ		±1σ		±1σ		±1σ		±1σ		$\infty 10^{-16}$	of total	±1σ			±2σ	
GUA 62-71 , whole rock, J ± 1σ = 1.1085 ± 0.001 (x10^{-3}). Location: 91.04° E, 15.10°N																	
0.9	46655.91	17.05	825.84	15.73	51.42	6.18	465.42	5.24	140.68	0.56	4.0	0.4	2.098	0.045	11.0	**12.17**	0.76
1.2	75017.09	23.44	3309.56	15.93	69.89	6.52	1522.25	5.29	181.79	0.52	16.2	1.8	1.713	0.010	28.7	**12.68**	0.24
1.5	98250.87	25.33	9999.04	18.18	139.19	6.31	3413.50	6.01	111.91	0.43	49.0	5.3	1.271	0.003	66.8	**12.81**	0.07
1.8	92109.22	27.23	11596.99	18.16	154.17	6.45	4045.85	6.11	63.62	0.34	56.8	6.2	1.300	0.003	80.2	**12.43**	0.05
2.1	105457.00	30.11	12412.77	19.07	165.06	6.24	4296.59	5.95	95.42	0.40	60.8	6.6	1.290	0.003	73.8	12.24	0.05
2.3	77517.56	23.44	8411.71	17.05	124.33	6.18	2936.32	5.73	86.14	0.40	41.2	4.5	1.301	0.004	67.7	12.17	0.07
2.5	61617.95	21.58	6167.51	15.82	66.12	6.18	2571.49	5.33	79.50	0.39	30.2	3.3	1.554	0.005	62.4	12.17	0.08
2.7	51375.51	19.74	4588.29	14.88	87.22	6.38	2166.49	5.79	77.52	0.37	22.5	2.4	1.761	0.007	56.0	12.23	0.10
3.0	99081.15	30.11	7134.81	16.68	131.35	6.24	2423.34	5.96	183.60	0.57	35.0	3.8	1.267	0.004	45.6	12.35	0.12
3.3	152069.10	42.77	9897.57	18.14	182.67	6.05	2518.24	5.53	304.28	0.79	48.5	5.3	0.949	0.003	41.1	12.32	0.14
3.6	147421.90	36.90	9051.87	16.65	182.18	6.45	1890.86	5.54	306.24	0.73	44.4	4.8	0.780	0.003	38.8	12.33	0.15
4.0	178389.50	43.76	10855.54	17.88	229.76	6.18	1927.31	5.19	370.39	0.79	53.2	5.8	0.663	0.002	38.8	12.44	0.15
5.0	363509.80	88.37	22586.24	24.62	440.98	6.32	3680.93	6.13	744.05	1.19	110.7	12.0	0.608	0.001	39.7	12.45	0.14
6.0	351163.20	79.41	23249.66	25.50	428.22	6.39	4523.01	6.13	684.77	1.09	113.9	12.4	0.727	0.001	42.6	12.54	0.13
6.0	103311.40	27.68	6941.79	15.85	132.28	6.04	1202.92	5.34	198.48	0.65	34.0	3.7	0.653	0.003	43.4	12.60	0.13
7.0	196150.70	45.01	13191.02	18.71	270.91	5.91	3083.53	6.13	374.66	0.84	64.7	7.0	0.881	0.002	43.8	12.70	0.13
8.0	221846.80	51.88	14539.20	19.31	293.01	6.11	2744.21	5.95	432.72	0.90	71.3	7.7	0.711	0.002	42.5	12.66	0.13
9.0	120639.10	33.01	8257.42	16.40	195.17	5.76	1769.90	5.73	227.08	0.65	40.5	4.4	0.809	0.003	44.6	12.71	0.13
10.0	21394.51	14.48	1577.50	14.49	83.58	6.03	331.10	5.92	37.47	0.25	7.7	0.8	0.792	0.016	48.5	12.82	0.18
12.0	88021.11	26.28	3332.18	15.29	87.16	6.39	823.69	5.67	223.26	0.61	16.3	1.8	0.933	0.008	25.2	12.97	0.28
Age Plateau =12.54 ± 0.04 Ma (steps 4.0 - 12.0 watts, 100% ^{39}Ar released)																	
GUA 110-11 , El Jute, whole rock, J ± 1σ = 1.1085 ± 0.001 (x10^{-3}). Location: N 14.975 °, W 89.803°																	
0.9	6343.83	12.38	490.28	14.14	0.00	5.78	97.01	5.04	15.32	0.18	2.4	0.7	0.748	0.043	28.8	**7.29**	0.32
1.2	63882.63	21.93	7995.93	16.92	133.81	6.31	2882.06	5.76	121.40	0.47	39.2	11.2	1.363	0.004	44.5	**6.94**	0.07
1.5	100472.40	29.41	14679.32	19.48	247.64	6.04	6674.09	7.15	167.19	0.63	71.9	20.6	1.719	0.003	51.7	**6.92**	0.06
1.8	71591.87	22.85	10970.59	17.92	152.85	5.85	8035.82	7.96	115.47	0.50	53.8	15.4	2.771	0.006	53.9	**6.87**	0.06
2.1	45699.08	19.24	7341.83	16.12	94.90	5.97	8734.57	7.77	72.35	0.33	36.0	10.3	4.502	0.011	55.8	**6.80**	0.05
2.3	22724.28	15.00	3804.11	15.99	35.91	6.10	6300.06	7.13	35.97	0.26	18.6	5.3	6.268	0.026	57.0	**6.67**	0.06
2.5	13569.04	14.21	2357.50	15.17	32.37	6.52	4867.93	6.70	21.07	0.20	11.6	3.3	7.817	0.049	59.0	**6.65**	0.08
2.7	11404.31	13.16	1956.86	15.14	27.25	6.10	4707.41	6.13	18.65	0.19	9.6	2.7	9.109	0.068	57.3	**6.55**	0.09
3.0	32089.96	15.81	4611.48	16.12	78.32	6.10	6950.11	7.42	59.19	0.34	22.6	6.5	5.708	0.020	48.5	**6.60**	0.07
3.3	20247.29	14.21	3049.27	15.25	22.34	6.10	5356.00	6.46	36.85	0.25	14.9	4.3	6.654	0.033	49.8	**6.48**	0.08
3.6	15359.52	14.21	2362.64	14.56	25.92	6.17	4942.23	6.85	27.81	0.23	11.6	3.3	7.927	0.048	50.9	**6.48**	0.08
4.0	7931.50	13.23	1289.55	16.42	33.46	6.45	3850.05	6.31	14.49	0.18	6.3	1.8	11.317	0.139	52.7	**6.35**	0.12
5.0	22077.14	15.81	3342.33	14.50	31.18	5.91	11942.34	9.76	43.98	0.25	16.4	4.7	13.547	0.058	48.5	**6.29**	0.08
6.0	27076.30	15.81	3750.92	15.35	56.37	6.24	13246.17	10.37	57.01	0.33	18.4	5.3	13.392	0.054	44.5	**6.30**	0.08
7.0	24259.69	15.00	3369.67	15.29	65.60	6.31	11752.32	9.70	50.20	0.32	16.5	4.7	13.230	0.059	45.5	**6.43**	0.09
Age Plateau =6.88 ± 0.03 Ma (steps 0.9 - 2.1 watts, 100% ^{39}Ar released)																	
GUA 110-12 , El Jute, whole rock, J ± 1σ = 1.1085 ± 0.001 (x10^{-3}), Location: N 14.975 °, W 89.803°																	
0.9	10389.23	14.34	1931.37	15.14	12.64	5.76	711.89	5.86	12.82	0.16	9.5	2.4	1.399	0.015	64.5	**6.78**	0.08
1.2	54869.72	19.33	13024.21	19.32	203.84	5.98	5340.98	6.84	38.51	0.29	63.8	16.4	1.557	0.003	80.6	**6.64**	0.03
1.5	66997.67	22.01	16332.39	20.80	253.15	6.13	4446.91	6.53	41.83	0.31	80.0	20.6	1.034	0.002	82.5	**6.61**	0.02
1.8	59050.30	22.01	14786.43	19.53	219.99	5.98	6389.84	7.74	36.04	0.28	72.5	18.7	1.642	0.003	83.5	**6.51**	0.02
2.1	35840.46	16.75	9168.86	17.28	118.34	5.76	8307.56	8.00	25.28	0.20	44.9	11.6	3.443	0.007	82.3	**6.30**	0.03
2.3	16460.64	14.34	4253.32	16.06	65.41	5.62	6406.31	7.00	13.03	0.16	20.8	5.4	5.725	0.022	82.0	**6.21**	0.04
2.5	8472.75	13.22	2189.91	15.16	21.19	5.55	4920.40	6.62	7.77	0.16	10.7	2.8	8.542	0.058	80.9	**6.13**	0.06
2.7	5293.31	13.37	1359.72	15.10	16.45	5.69	4271.08	6.37	5.43	0.14	6.7	1.7	11.945	0.128	80.8	**6.17**	0.09
3.0	6828.58	13.59	1736.71	14.09	21.34	5.83	6534.75	7.16	7.56	0.14	8.5	2.2	14.312	0.112	80.5	**6.21**	0.07
3.3	4461.97	12.32	1109.13	15.08	19.06	5.76	4488.93	6.34	4.87	0.14	5.4	1.4	15.398	0.201	81.6	**6.45**	0.12
3.6	2763.87	13.01	685.88	14.45	0.00	5.69	2570.97	5.99	3.19	0.11	3.4	0.9	14.265	0.288	78.6	**6.22**	0.16
4.0	2597.88	12.59	617.35	15.72	11.03	5.83	2304.89	5.90	2.64	0.10	3.0	0.8	14.212	0.346	82.2	**6.79**	0.20
5.0	3652.92	13.22	896.48	15.08	0.00	5.83	3655.89	6.41	4.27	0.12	4.4	1.1	15.528	0.250	79.2	**6.34**	0.14
6.0	6181.84	13.59	1484.47	14.30	13.35	5.34	6221.75	7.16	8.07	0.15	7.3	1.9	15.963	0.148	75.3	**6.16**	0.09
7.0	8639.62	13.37	1745.69	14.03	0.00	5.98	8344.11	8.34	14.04	0.17	8.6	2.2	18.209	0.141	65.3	**6.35**	0.09
8.0	19248.87	13.90	2623.87	14.49	32.40	5.83	8739.79	8.24	40.29	0.25	12.9	3.3	12.782	0.069	44.5	**6.40**	0.09
9.0	18078.51	12.97	2527.48	14.48	25.23	6.17	8201.38	7.90	36.68	0.28	12.4	3.2	12.455	0.070	46.3	**6.50**	0.10
8.0	5892.63	11.81	1347.63	15.10	19.21	6.18	6417.48	6.51	8.27	0.14	6.6	1.7	18.287	0.196	73.7	**6.33**	0.10
9.0	12855.89	13.90	1383.36	15.10	18.35	5.98	6506.37	7.19	30.89	0.26	6.8	1.7	18.066	0.189	36.0	**6.58**	0.16

Table S1-2. Heating step releases and statistics for the calculation of whole rock basalt $^{40}Ar/^{39}Ar$ ages.

Supplement 2. Terrestrial ^{10}Be measurements and conversion to erosion rates

Sediment grain sizes were separated using a phi-scale sieve set. Fractions coarser than 2 mm were crushed and sieved to obtain a 0.25-0.5 mm powder. Quartz isolation, purification and dissolution, ion exchange extraction and precipitation of beryllium were performed following an adaptation of the technique of (Kohl and Nishiizumi 1992). A ^{9}Be carrier (Scharlau BE03450100 carrier batch 2Q2P – 14/10/10) with a measured $^{10}Be/^{9}Be$ ratio of $1.5x10^{-15}$ was added to each sample. Beryllium hydroxide was precipitated at pH 8-9, oxidized to BeO over an open butane-propane flame and mixed with Nb powder. The $^{10}Be/^{9}Be$ ratio was measured by accelerator mass spectrometry (AMS) at PRIME lab, Purdue University. Results were normalized to the 07KNSTD standard (Nishiizumi, Imamura et al. 2007) with an assumed $^{10}Be/^{9}Be$ ratio of 2.79×10^{-11} (Balco 2009). The $^{10}Be/^{9}Be$ ratios of the procedural blanks ranged from $1.6\pm0.4 \times10^{-15}$ to $7.1\pm1.5x10^{-15}$ (mean $2.0 \pm0.5 \times10^{-15}$, n=4). Reported one-sigma uncertainties (Table B1) encompass uncertainties on Purdue AMS measurement, uncertainty on the primary standard, and uncertainties on blank corrections.

Soil/rock Sample [1]	Easting	Northing	Elevation	Quartz used	[^{10}Be]	Shielding factor[2]	P_μ [3]	P_{spal} [3]	Integrated wet bulk density[4]	Erosion Rate[5]	Quartz enrichment factor[4]	Erosion Rate[5]	Erosion Rate Below Upland surface
	(°)	*(°)*	*(m)*	*(g)*	*(10^4 at g^{-1})*		*(at g^{-1} yr^{-1})*	*(at.g^{-1} yr^{-1})*	*(g cm^{-3})*	*m/My*		*m/My*	*m/My*
CLP1 (47-61)r*	-89.621	15.149	2,610	?	41.2 ± 1.2	0.97	0.41	16.6	2.6 ± 0.1	27.6 ± 2.6	1.0 ± 0.0	27.6 ± 2.6	0 ± 4
CLP2 (47-62)r*	-89.621	15.149	2,610	?	34.2 ± 1.1	0.97	0.41	16.6	2.6 ± 0.1	32.9 ± 3.1	1.0 ± 0.0	32.9 ± 3.1	0 ± 4
SM1 (10-53)s°	-89.687	15.132	2,275	10.60	146.3 ± 13.5	0.92	0.37	13.0	1.6 ± 0.2	11.2 ± 2.1	1.0 ± 0.0	11.2 ± 2.1	12 ± 4
SM2 (10-52)s°	-89.687	15.132	2,275	29.38	20.1 ± 4.2	0.92	0.37	13.0	1.6 ± 0.2	78.5± 20.9	1.4 ± 0.3	110 ± 38	12 ± 4
SM3 (47-101)s*	-89.645	15.124	1,875	?	13.4 ± 0.6	0.92	0.33	10.1	1.6 ± 0.2	84.1 ± 13.2	1.4 ± 0.3	118 ± 31	41 ± 4

Table S2-1. Soil ^{10}Be samples locations, concentrations and environmental parameters. [1] Sample type: s: soil, r: rock. Standard used: *: 07KNSTD, °: KNSTD [2]: combination of topographic obstruction and vegetation shielding. [3] Production rates for neutrons (P_{spal}) and muons (P_μ), calculated using the CRONUS calculator for a polar sea-level ^{10}Be production rate of 5.1 at.g^{-1}.y^{-1} (Balco, Stone et al. 2008), for indicated shielding factor. [4] Quartz enrichment and soil density from published measurements in similarly eroding tropical soils and saprolite (White, Blum et al. 1998, Ferrier, Kirchner et al. 2010, Brocard, Willenbring et al. 2015). [5] CRONUS-calculated using time-dependent ^{10}Be production rate (version 2.3, constants version 2.3, muons version 1.1).

Stream[1]	Easting	Northing	Quartz used	[^{10}Be]	Quartz-bearing[2] lithologies	A_{Qz} Average Elevation[3]	Denudation Rate Unweighted [3,5]	Denudation Rate weighted [5, 6]	Denudation Rate Qz enrichment	Erosion Below Upland surface
	(°)	*(°)*	*(g)*	*(10^4 at g^{-1})*	*(% total catchment)*	*(m)*	*(m/Myr)*	*(m/Myr)*	*(m/Myr)*	*(m/Myr)*
COL (SM)*	-89.644	15.124	32.41	126.84 ± 2.09	CU(100)	2,122	11.0 ± 1.7	11.0 ± 1.7	15 ± 4	24 ± 4
FRI (SM)*	-89.650	15.109	27.23	24.37 ± 0.66	CU(100)	2,050	54.3 ± 8.4	54.3 ± 8.4	76 ± 20	28 ± 4
SLO (SM)*	-90.183	14.957	16.85	6.90 ± 0.34	CU(100)	1,892	163 ± 26	163 ± 26	228 ± 61	35 ± 4
RAN (SM)*	-89.655	15.030	32.56	5.94 ± 0.31	CU(70)	915	108 ± 10	101 ± 11	142 ± 34	60 ± 4
SCO (SM)*	-90.101	15.104	28.31	25.84 ± 0.51	CU(81)	2,014	67.9 ± 6.7	63.9 ± 6.7	90 ± 21	38 ± 4
SIM (SM)*	-90.169	15.112	45.18	21.46 ± 0.90	CU(95)	1,856	54.4 ±5.8	51.2 ± 5.7	72 ±17	26 ± 4
SBM (SM)*	-90.182	15.079	42.55	27.56 ± 1.12	CU(100)	1,695	38.0 ± 6.0	38.4 ± 6.0	54 ±14	45 ± 4
MOR (SC)*	-90.183	14.957	17.97	9.82 ± 0.37	CU(81)SR(2)	1,122 (1,213)	77.7 ± 11.4	73.8 ± 11.3	103 ± 27	61 ± 4
SALS (SC)*	-90.282	15.061	33.66	21.14 ± 0.48	CU(92)QP(8)	1,330 (1,304)	39.9 ± 6.2	40.5 ± 6.2	57 ± 15	73 ± 4
SALI (SC)*	-90.304	15.095	33.05	15.36 ± 0.34	CU(63)QP(25)SR(12)	1,326 (1,243)	52.7 ± 8.3	55.4 ± 8.4	73 ± 17	71 ± 4
SMS (SC)°	-90.382	15.025	26.15	19.50 ± 0.38	CU(100)	1,707	50.2 ± 7.6	50.2 ± 7.6	70 ± 19	50 ± 4
SMM (SC)*	-90.388	15.062	51.13	21.00 ± 0.32	CU(100)	1,611	48.7 ± 7.4	48.7 ± 7.4	68 ± 18	58 ± 4
SMI (SC)°	-90.382	15.148	30.62	20.63 ± 0.11	CU(69)QP(22)SR(9)	1,391 (1,292)	44.6 ± 7.0	47.3 ± 7.1	69 ± 17	66 ± 4
SGA (SC)*	-90.406	15.148	43.49	24.67 ± 0.41	CU(43)QP(18)SR(69)	1,172 (1,127)	30.6 ± 4.8	31.5 ± 4.8	44 ± 12	77 ± 4
PAT (SC)°	-90.557	15.145	30.09	14.65 ± 0.43	CU(55)SR(45)	1,224 (1,330)	63.5 ± 9.2	59.7 ± 9.1	84 ± 22	76 ± 4
ECS (SC)°	-90.559	14.992	15.01	20.84 ± 5.20	CU(91)	1,974	64.6 ± 20.0	64.6 ± 20.0	90 ± 34	38 ± 4
COT (SC)°	-90.616	14.905	20.29	17.89 ± 0.61	CU(100)	1,637	61.9 ± 9.6	61.9 ± 9.6	87 ±23	71 ± 4
XEU (SC)°	-90.603	15.058	50.22	7.08 ± 0.28	CU(100)	1,746	162 ± 25	162 ± 25	227 ± 60	55 ± 4
CUB (SC)*	-90.592	15.123	35.64	8.24 ± 0.27	CU(88)QP(11)	1,432 (1,389)	103 ± 15	106 ± 16	148 ± 39	73 ± 4
PAC (SC)°	-90.646	15.155	33.28	10.77 ± 0.28	CU(98)SR(2)	1,211 (1,213)	80.2 ± 12.1	80.2 ± 12.1	112 ± 29	67 ± 4
PAS (SC)*	-90.681	15.090	32.13	10.27 ± 0.25	CU(100)	1,947	112 ± 17	112 ± 17	157 ± 41	38 ± 4
PAE (SC)*	-90.707	15.125	26.01	7.31 ± 0.26	CU(100)	1,779	146 ± 22	146 ± 22	204 ± 54	50 ± 4
CHI (SC)*	-90.761	15.158	15.12	28.90 ± 0.75	CU(100)	1,838	40.0 ± 6.2	40.0 ± 6.2	56 ± 14	40 ± 4
SAC (SC)*	-90.911	15.153	12.04	17.76 ± 0.54	CU(100)	1,865	65.8 ± 10.1	65.8 ± 10.1	92 ± 24	47 ± 4
XOL (SC)*	-91.002	15.144	20.95	13.80 ± 0.62	CU(97)QP(3)	1,889 (1,890)	84.2 ± 13.3	85.4 ± 13.4	113 ± 28	40 ± 4
ACA (SC)°	-90.914	15.206	20.09	12.88 ± 0.38	CU(83)QP(17)	1,635 (1,570)	81.5 ± 8.5	84.6 ± 12.9	118 ± 31	54 ± 4
CATA (CH)*	-91.130	15.495	55.62	26.56 ± 1.07	SR(18)TS(22)QP(7)	1,944 (1,880)	44.1 ± 7.1	45.7 ± 7.2	64 ± 17	98 ± 4
CHEL (CH)*	-91.129	15.504	50.65	13.49 ± 0.48	SR(25)TS(20)QP(3)	2,102 (2,027)	88.6 ± 9.5	92.2 ± 14.3	129 ± 34	95 ± 4
SUM (CH)*	-91.129	15.495	35.37	3.68 ± 0.17	SR(73)TS(14)	1,885 (1,820)	284 ± 32	294 ± 46	412 ± 109	90 ± 4
IXT (CH)*	-91.089	15.621	44.45	2.99 ± 0.13	SR(93)TS(6)	1,602 (1,720)	333 ± 34	310 ± 48	434 ± 115	116 ± 4
XAC (CH)*	-91.087	15.619	15.38	4.04 ± 0.35	SR(50)TS(16)QP(2)	2,041 (1,923)	258 ± 32	274 ± 47	384 ± 105	96 ± 4

Table S2-2. ^{10}Be concentrations and environmental parameters used for the calculation of catchment-wide erosion rates

[1] Sample location: SM: Sierra de las Minas, SC: Sierra de Chuacús, CH: Cuchumatanes Highs. Standard used: *: 07KNSTD, °: KNSTD. [2] Weighting of lithologies in subsequent calculations as follows, normalized to Chuacús (CH): SR. Santa Rosa Fm. (0.4), QP: Quaternary pumice (0.1), Todos Santos Fm. (0.6). [3] Values after applying the quartz-content weighting. [4] Production rates for neutrons (P_{spal}) and muons (P_{μ}), calculated using the CRONUS calculator for a polar sea-level ^{10}Be production rate of

5.1 at·g^{-1}·y^{-1} (Balco, Stone et al. 2008), for the indicated topographic shielding and vegetation shielding of 7%. [5] Calculated using ground densities and quartz enrichment factor as for soils in Table SI-21, using the CHRONUS time-depend production rate scheme [6] No weighting according to quartz content for quartz-bearing lithologies.

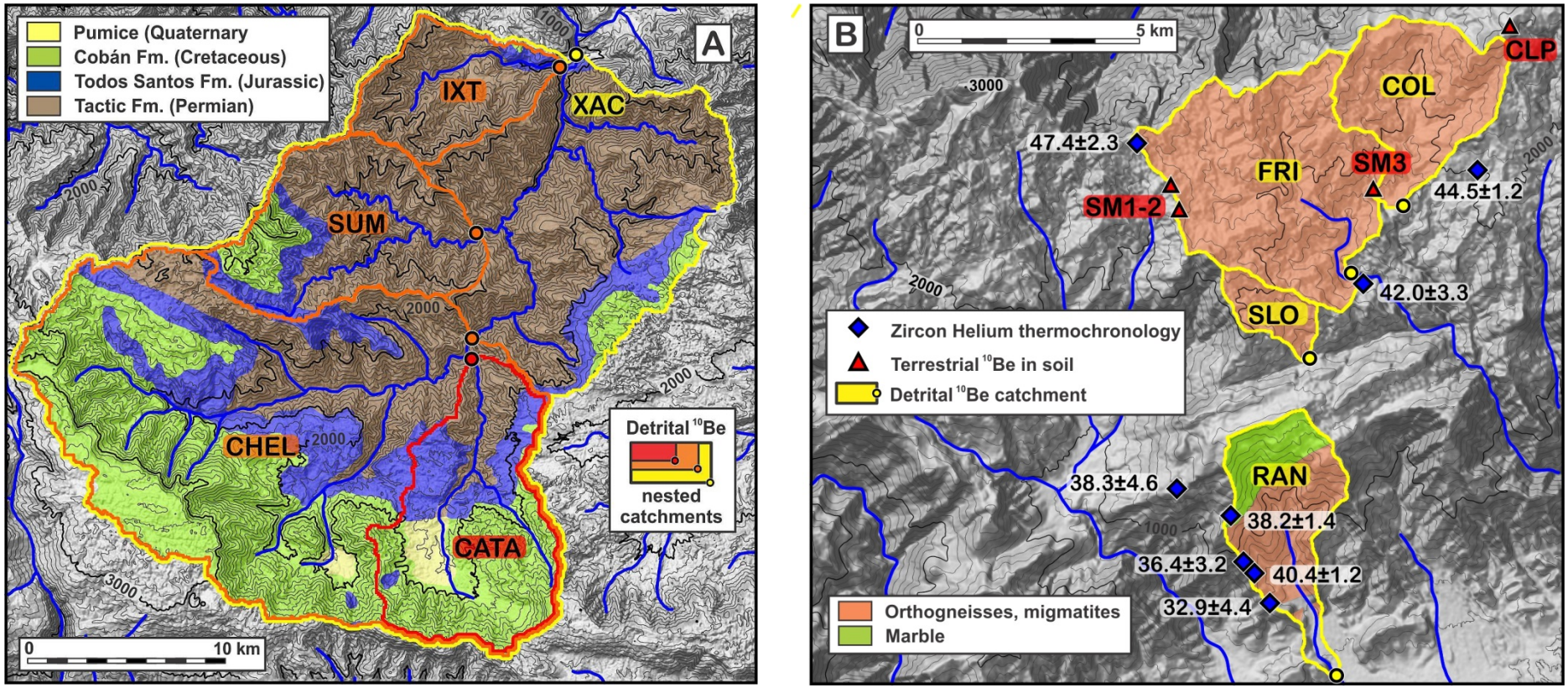

Figure S2-3. Detrital ^{10}Be catchments lithology. (a): Altos de Cuchumatanes (CATA: Catarata, CHEL: Chel, IXT: Ixtahuacan, SUM: Sumalá, XACB: Xacbal), (b): Sierra de las Minas (COL: Colorado, FRI: Frío, RAN: Quebrada Ranchitos/In situ: CLP: Cerro las Palomas, SM: Sierra de las Minas). Zircon data from (Simon-Labric, Brocard et al. 2013)

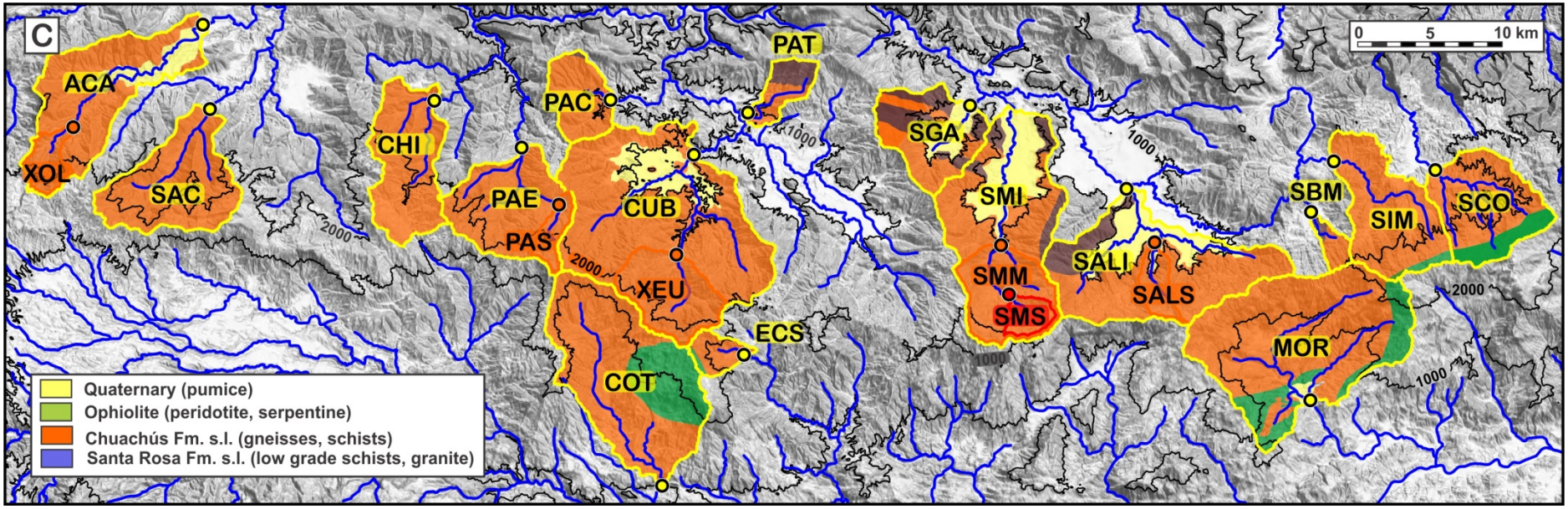

(c): Sierra de Chuacús (ACA: Agua Caliente, CHI:, COT: Cotón, CUB: Cubulco, ECS: El Chol Superior, MOR: Morazán, PAC: Pacani, PAE: Paguoza East, PAS: Paguoza South, PAT: Patixla, SAC: Sacaj, SALI: Salamá Inferior, SALS: Salamá Superior, SBM: Santa Barbara Modern, SCO: Chilasco, SGA: San Gabriel, SIM: San Isidro Modern, SMI: San Miguel Inferior, SMM: San Miguel Medio, SMS: San Miguel Superior, XEU: Xeúl, XOL: Xoljá).

References

Balco, G. (2009). "26Al-10Be exposure age/erosion rate calculators: update from v. 2.1 to v. 2.2." CRONUS Online Calculator, http://hess.ess.washington.edu.

Balco, G., et al. (2008). "A complete and easily accessible means of calculating surface exposure ages or erosion rates from (10)Be and (26)Al measurements." Quaternary Geochronology **3**(3): 174-195.

Brocard, G. Y., et al. (2015). "Effects of a tectonically-triggered wave of incision on riverine exports and soil mineralogy in the Luquillo Mountains of Puerto Rico." Applied Geochemistry **63**: 586-598.

Ferrier, K. L., et al. (2010). "Mineral-specific chemical weathering rates over millennial timescales: Measurements at Rio Icacos, Puerto Rico." Chemical Geology **277**(1-2): 101-114.

Kohl, C. P. and K. Nishiizumi (1992). "CHEMICAL ISOLATION OF QUARTZ FOR MEASUREMENT OF INSITU-PRODUCED COSMOGENIC NUCLIDES." Geochimica et Cosmochimica Acta **56**(9): 3583-3587.

Nishiizumi, K., et al. (2007). "Absolute calibration of 10 Be AMS standards." Nuclear Instruments and Methods in Physics Research Section B: Beam Interactions with Materials and Atoms **258**(2): 403-413.

Simon-Labric, T., et al. (2013). "Preservation of contrasting geothermal gradients across the Caribbean-North America plate boundary (Motagua Fault, Guatemala)." Tectonics: n/a-n/a.

White, A. F., et al. (1998). "Chemical weathering in a tropical watershed, Luquillo Mountains, Puerto Rico: I. Long-term versus short-term weathering fluxes." Geochimica et Cosmochimica Acta **62**(2): 209-226.

Supplement 3. Stream segmentation using LSDTopoTools

We analyzed longitudinal channel profiles using the statistical approach of (Mudd, Attal et al. 2014) implemented using LSDTopoTools, which identifies locations where either erodibility or erosion rates are most likely to change. The software recursively tests possible various combinations of contiguous segments along the selected rivers (Table S3-1), allowing identification of most likely m/n ratio of each river, the statistically most likely number of linearized segments, and their extent (Fig. S3-2). The statistical analysis is performed over after 300 iterations of the segment finding algorithm, and for m/n ratio varying at 0.25 intervals over a range from 0.1 to 0.9. The averaged m/n ratio of the investigated subset of rivers is 0.48 ± 0.11.

Rivers	Best estimate m/n ratio	STD AICc value	Rivers	Best estimate m/n ratio	STD AICc value
Blanco	0.525	130.522	Las Canoas	0.550	31.3209
Cacuj	0.525	209.432	Pagueza	0.500	28.1190
Chibalam-Yerbabuena	0.675	177.548	Quillila-Carchela	0.675	85.8668
ChitapolC	0.625	262.905	Rabinal	0.450	90.7101
ChitapolE	0.500	62.5817	Sacaj	0.450	112.203
Chixoy	0.375	152.800	Salama	0.600	6.53611
Cucul	0.500	65.7579	San Miguel	0.475	160.916
Ekca-Xecam-Chilil	0.350	158.868	Sicache	0.300	412.876
El Molino	0.350	303.865	Xeul	0.550	56.9638
Las Barras	0.325	4.66082			

Table S3-1. Results from statistical method based on the corrected Akaike Information Criterion (AICc) presenting the best estimate m/n ratio for selected rivers in the region. The statistical analysis is running for the main stem and standard deviation of the AICc values are measured after 300 iterations of the segment finding algorithm (Mudd, Attal et al. 2014).

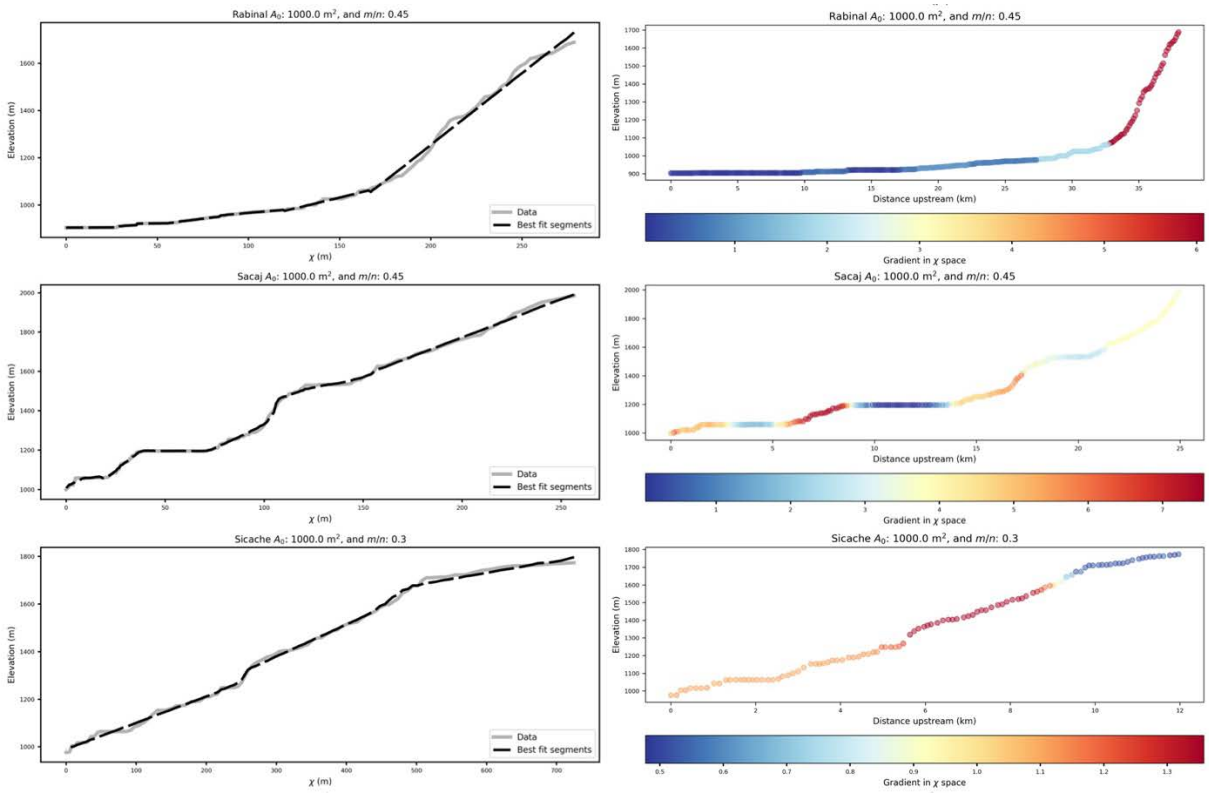

Figure S3-2. Left: segment fitting for three examples of river profiles using the best estimate m/n ratio from the statistical analysis presented in Table SI-31. Right: channel profiles colored by the best fit slope in χ-elevation space.

Mudd, S. M., et al. (2014). "A statistical framework to quantify spatial variation in channel gradients using the integral method of channel profile analysis." Journal of Geophysical Research: Earth Surface **119**(2): 138-152.

Supplement 4. Knickpoints and segments classification

Table S4-1. River segments and knickpoints (excel file).

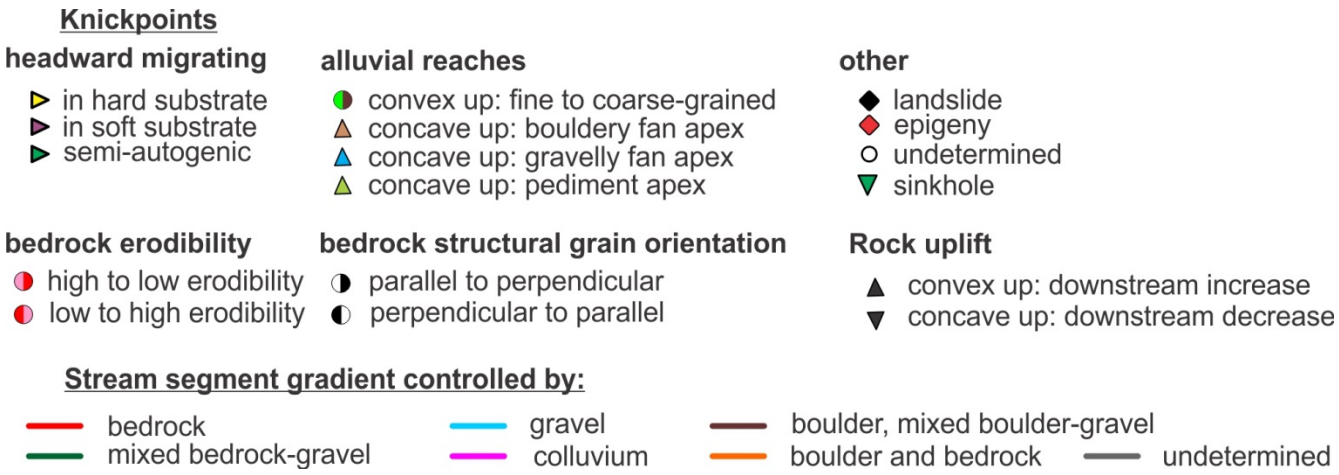

Legend of figures S4-2 to S4-6.

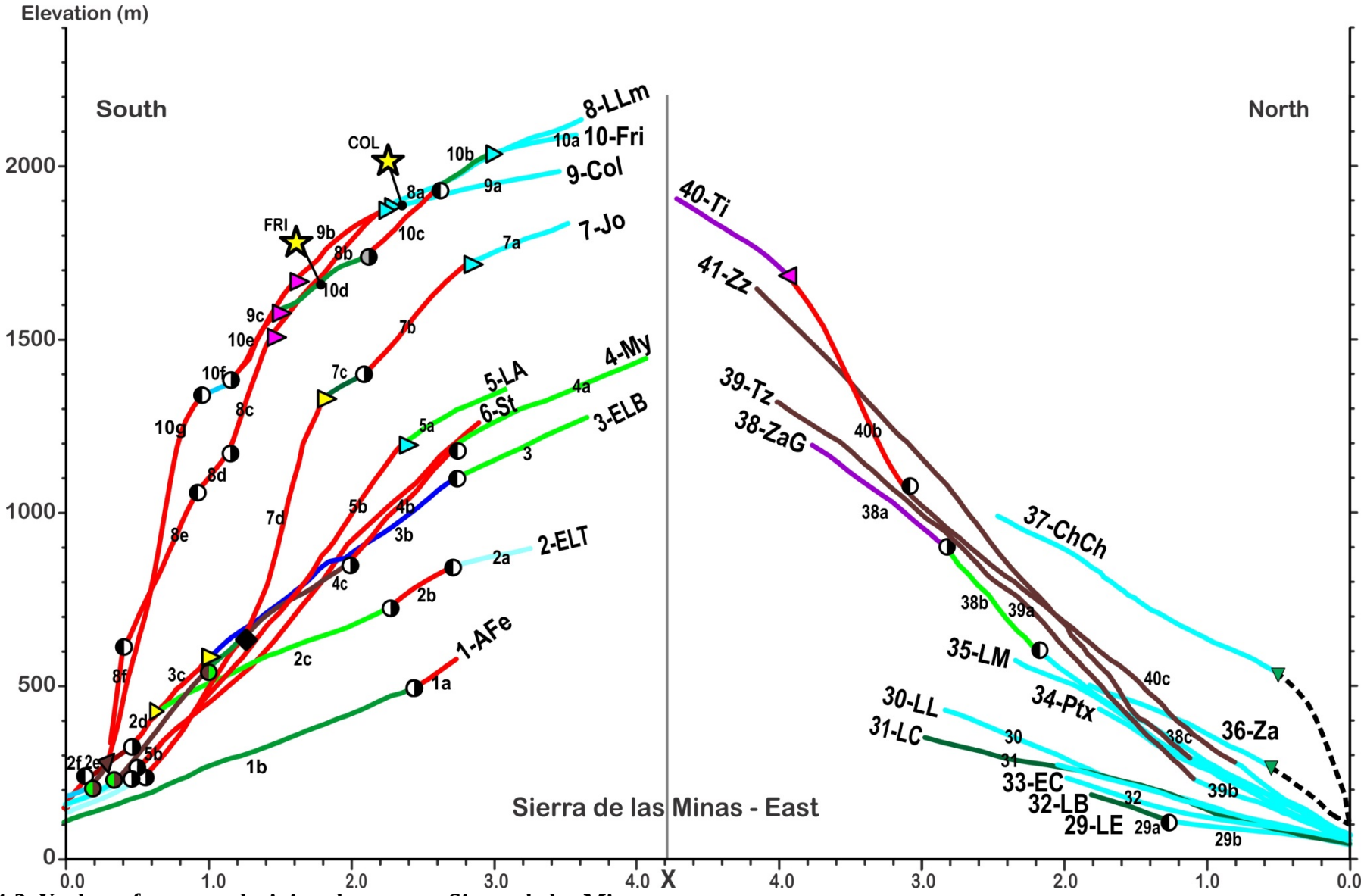

Figure S4-2. X-plots of streams draining the eastern Sierra de las Minas.
Stream names: Southern flank: 1-AFe: Agua Fría east; 2-ELT: El Lobo-Tinto; 3- ELB: El Lobo-Blanco; 4-My: Mayuelas, 5-LA: Los Achiotes, 6-St: Santiago, 7-Jo: Jones, 8-LLm: La Lima, 9-Col: Colorado, 10-Fri: Agua Fría. Northern flank: 29-LE: Los Espinos, 30-LL: Los Limones, 31-LC: Las Cañas, 32-LB: Las Balandras, 33-EC: El Chapín, 34-Ptx: Pataxte, 35-LM: Las Minas, 36-Za: Zarquito, 37-ChCh: river on carbonates ending in sinkhole, 38-ZaG: Zarco Grande, 39-Tz: Tze, 40-Ti: Tinajas, 41-Zz: Zarzaparillas. Yellow stars: sampling sites for detrital ^{10}Be erosion rate measurements.

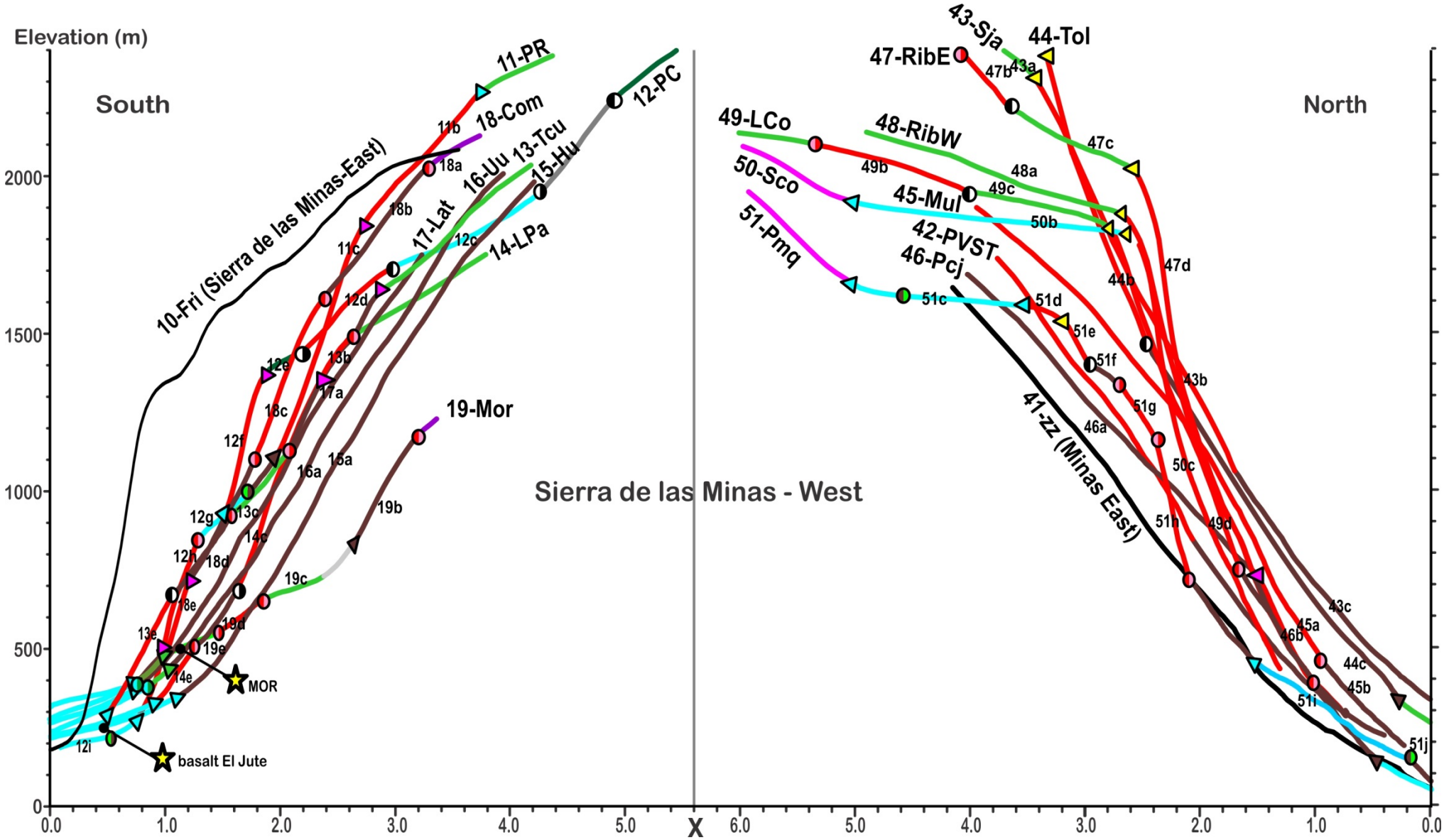

Figure S4-3. χ- plot of streams draining the western part of the Sierra de las Minas.

Stream names : Southern flank: 11-PE: Pasabien Repollal, 12-PC: Pasabien-Chorro, 13-Tcu: Teculutan, 14-LPa: La Palmilla, 15-Hu: Huijo, 16-Uu: Uyus, 17-Lat: Lato, 18-Com: Comaja, 19-Mor: Morazán. Northern flank: 41-Zz: Zarzaparilla, 42-PVST: Pueblo Viejo-Santo Toribio, 43-Sja: Samilija, 44-Tol: Toila, 45-Mul, Mululjá, 46-Pcj: Pancajoc, 47-RibE: Ribaco east, 48-RibW: Ribaco west, 49-LCo: La Concepción, 50-Sco: Chilasco, 51-Pmq: Panimaquito. Yellow stars: sampling sites for detrital ^{10}Be erosion rate measurements.

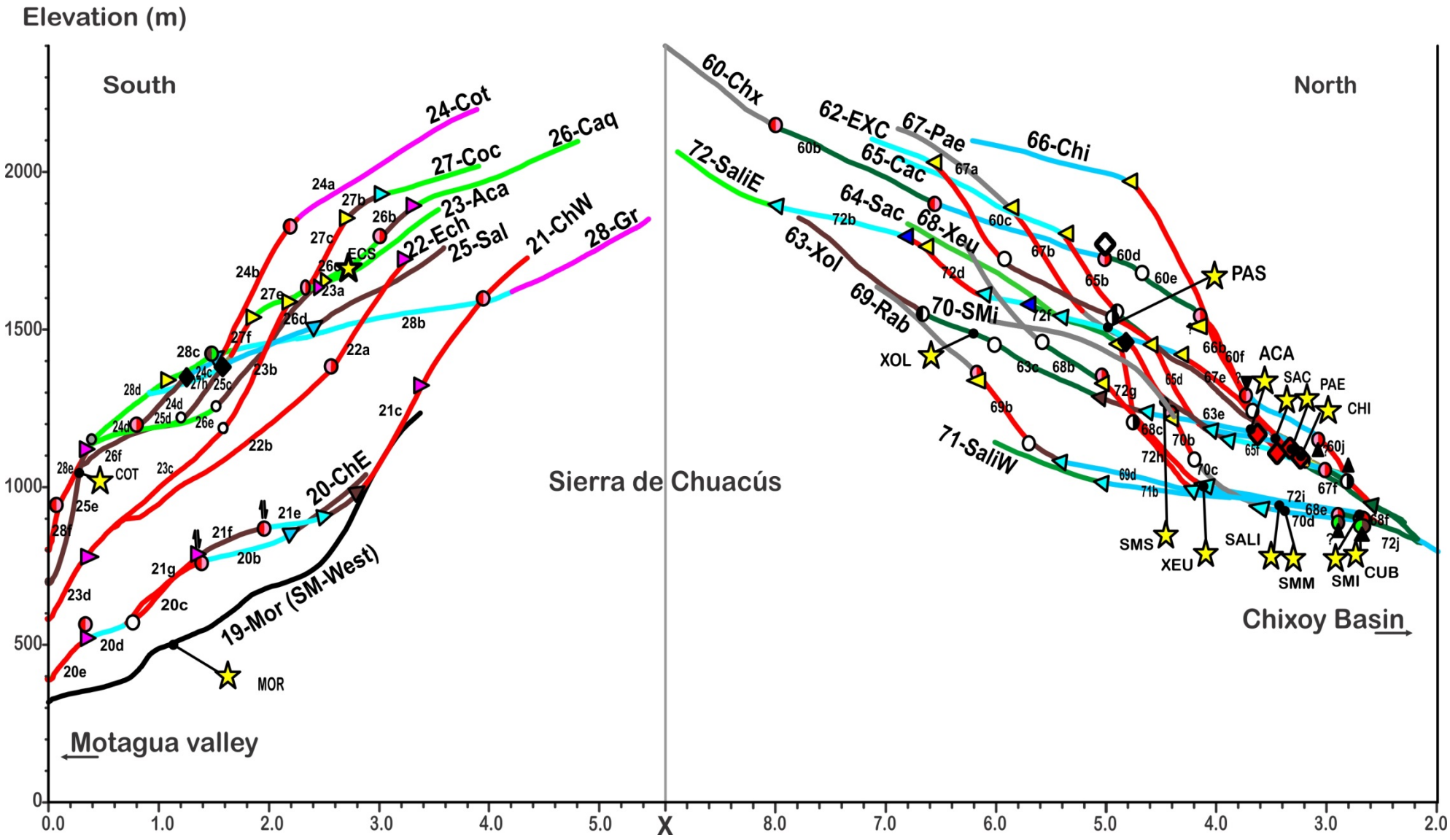

Figure S4-4. χ-plot of streams draining the Sierra de Chuacús.
Stream names: Southern flank: 20-ChE: Chuacús East, 21-ChW: Chuacús west, 22-ECh: El Chol, 23-Aca: Agua Caliente, 24-Cot: Cotón, 25-Sal: Saltán, 26-Caq: Caquíl, 27- Coc: Cocol, 28-Gr: Grande. Northern flank: 72-SaliE: Salamá East, 71-SaliW: Salamá West, 70-SMi: San Miguel, 69-Rab: Rabinal, 68-Xeu: Xeul, 67-Pae: Pagueza, 66-Chi: Chiabalam-Yerbabuena, 65-Cac: Cacúj, 64-Sac: Sacaj, 63-Xol: Xoljá, 62-EXC: Ekca-Xecam-Chilil, 61: Cuc: Cucul, 60-Chx: Chixóy. Yellow stars: sampling sites for detrital ^{10}Be erosion rate measurements.

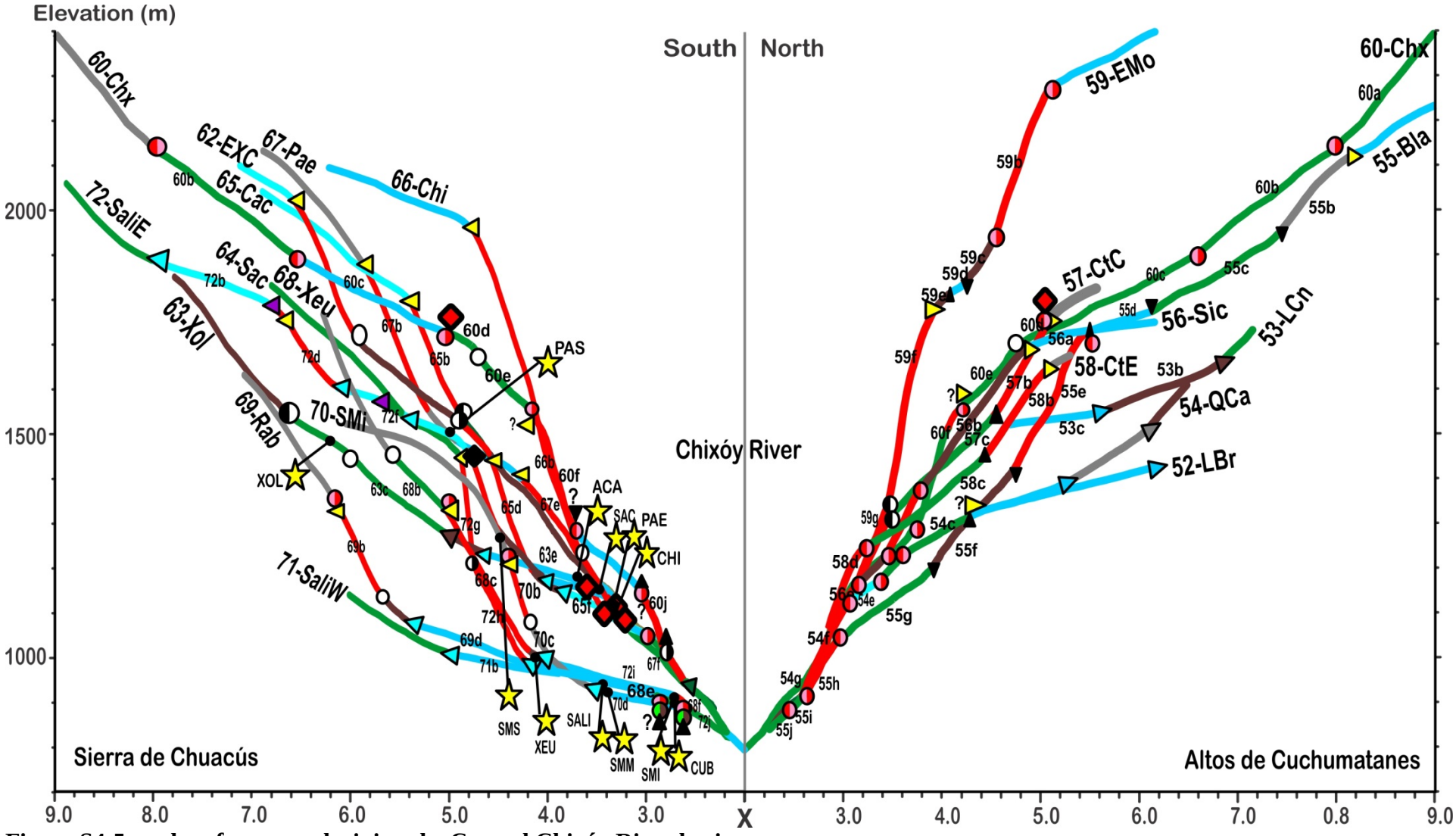

Figure S4-5. χ-plot of streams draining the Central Chixóy River basin

Stream names: Southern flank: 72-SaliE: Salamá East, 71-SaliW: Salamá West, 70-SMi: San Miguel, 69-Rab: Rabinal, 68-Xeu: Xeul, 67-Pae: Pagueza, 66-Chi: Chiabalam-Yerbabuena, 65-Cac: Cacúj, 64-Sac: Sacaj, 63-Xol: Xoljá, 62-EXC: Ekca-Xecam-Chilil, 61: Cuc: Cucul, 60-Chx: Chixóy.
Northern flank: 52-LBr: Las Barras, 53-LCa: Las Canoas, 54-QCa: Quililá-Carchela, 55-Bla: Blanco, 56-Sic: Sicaché, 57-Ctc: Chitapol Centre, 58: CtE: Chitapol East, 59-EMo: El Molino 60-Chx: Chixóy. Yellow stars: sampling sites for detrital ^{10}Be erosion rate measurements.

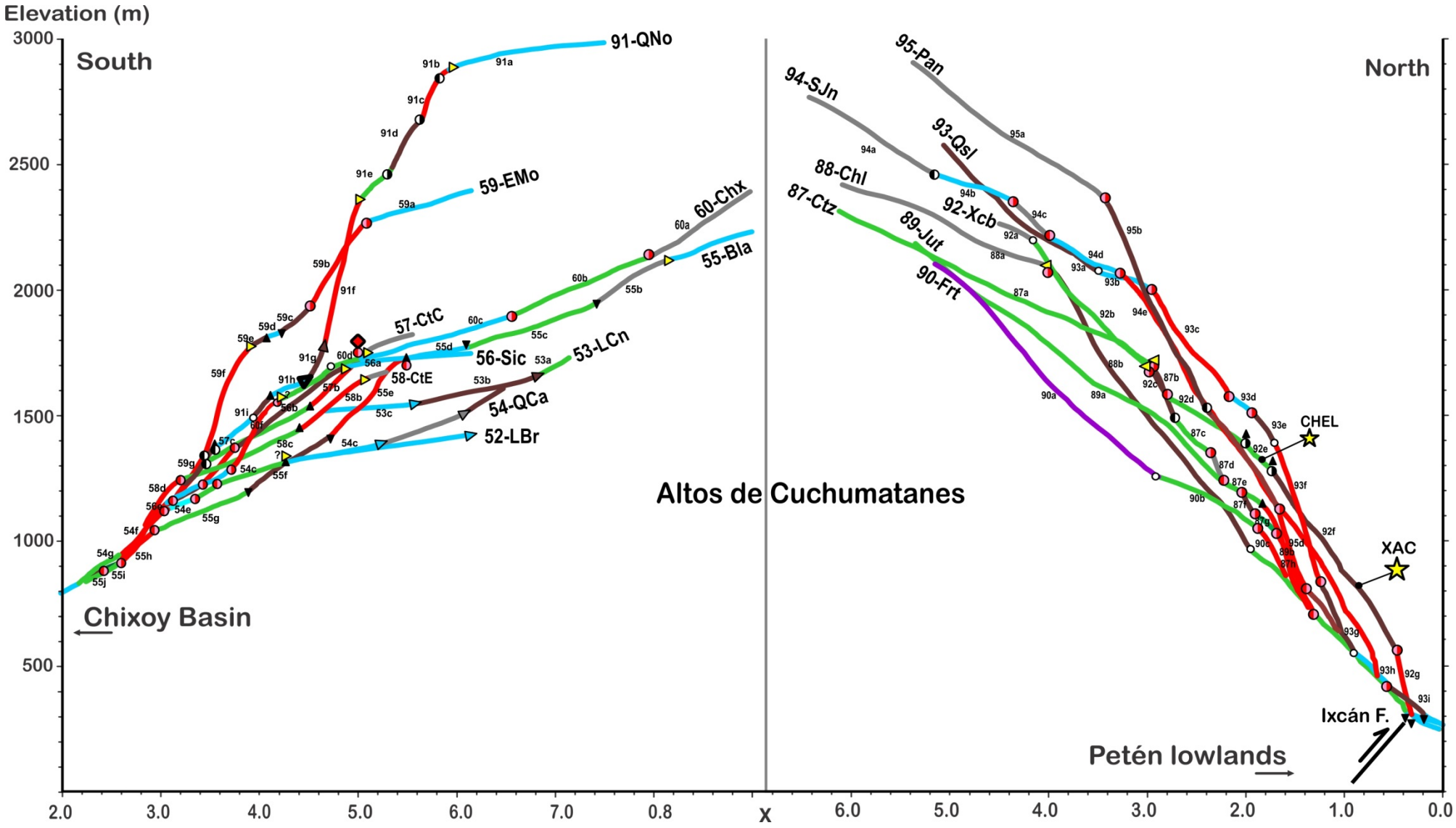

Figure S4-6. χ-plot of streams draining the Altos de Cuchumatanes along a N-S transect
Stream names: Southern flank: 52-LBr: Las Barras, 53-LCa: Las Canoas, 54-QCa: Quililá-Carchela, 55-Bla: Blanco, 56-Sic: Sicaché, 57-Ctc: Chitapol Centre, 58: CtE: Chitapol East, 59-EMo: El Molino 60-Chx: Chixóy.
Northern flank: 87-Ctz: Cotzal, 88-Chl: Chel, 89-Jut: El Jute, 90-Frt: unnamed frontal stream, 91- QNo: Quilén Novillo, 92- Xcb: Xacbal, 93- Qsl: Quisil, 94-SJn: San Juan, 95- Pan: Panila. Yellow stars: sampling sites for detrital ^{10}Be erosion rate measurements.

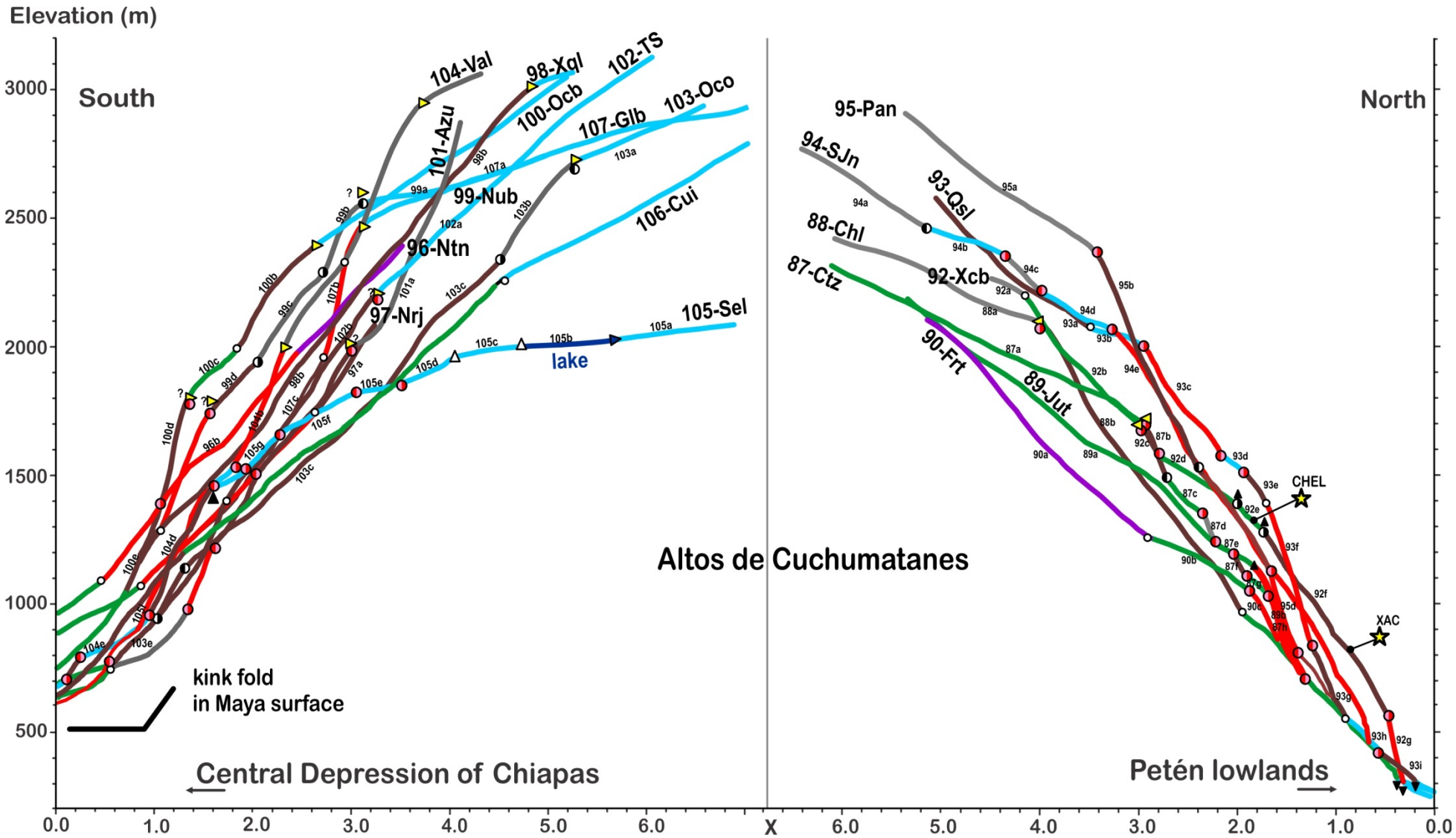

Figure S4-7. χ-plot of streams draining the Altos de Cuchumatanes along an W-E transect

Stream names: Northern flank: 87-Ctz: Cotzal, 88-Chl: Chel, 89-Jut: El Jute, 90-Frt: unnamed frontal stream, 91- QNo: Quilén Novillo, 92- Xcb: Xacbal, 93-Qsl: Quisil, 94-SJn: San Juan, 95- Pan: Panila.

Eastern flank: 96-Ntn: Nenton, 97- Nrj: Naranjo, 98- Xql: Xoquil, 99-Nub: Nubila, 100-Ocb: Ochebal-Catarina, 101-Azu: Azul, 102-TS: Todos Santos, 103-Oco: Ocho, 104-Val: Valparaiso, 105-Sel: Selegua, 106-Cui: Cuilco. Yellow stars: sampling sites for detrital ^{10}Be erosion rate measurements.